Received: 02 February 2022 | Revised: 26 July 2022 | Accepted: 03 August 2022

DOI: 10.1002/hep.32746

ORIGINAL ARTICLE

OPEN

Janus kinase 2 inhibition by pacritinib as potential therapeutic target for liver fibrosis

Sandra Torres[1,2,3] | Cristina Ortiz[1] | Nadine Bachtler[1] | Wenyi Gu[1,4] | Leon D. Grünewald[5] | Nico Kraus[1] | Robert Schierwagen[1,4] | Christoph Hieber[1] | Caroline Meier[1] | Olaf Tyc[1] | Maximilian Joseph Brol[1,4] | Frank Erhard Uschner[1,4] | Bart Nijmeijer[6] | Christoph Welsch[1] | Marie-Luise Berres[7] | Carmen Garcia-Ruiz[2,3,8] | Jose Carlos Fernandez-Checa[2,3,8] | Christian Trautwein[7] | Thomas J. Vogl[5] | Stefan Zeuzem[1] | Jonel Trebicka[1,4,9] | Sabine Klein[1,4]

[1]Department of Internal Medicine I, Goethe University Clinic Frankfurt, Frankfurt, Germany

[2]Department of Cell Death and Proliferation, Instituto Investigaciones Biomédicas de Barcelona (IIBB), Spanish National Research Council (CSIC), Barcelona, Spain

[3]Liver Unit-IDIBAPS and Centro de Investigación Biomédica en Red (CIBERehd), Barcelona, Spain

[4]Department of Internal Medicine B, University of Münster, Münster, Germany

[5]Department of Diagnostic and Interventional Radiology, Universit+y Hospital Frankfurt, Frankfurt am Main, Germany

[6]Research and Development Department, Linxis BV, Amsterdam, The Netherlands

[7]Department of Internal Medicine III, Aachen University Hospital, Aachen, Germany

[8]Department of Medicine, University of Southern California, Research Center for Alcoholic Liver and Pancreatic Diseases and Cirrhosis, Keck School of Medicine, University of Southern California, Los Angeles, California, USA

[9]European Foundation for the Study of Chronic Liver Failure – EF Clif, Barcelona, Spain

Correspondence
Jonel Trebicka, Department of Internal Medicine B, University of Münster, Westfälischen Wilhelms-Universität Münster, Albert-Schweitzer-Campus 1, Gebäude A1, 48149 Münster
Email: jonel.trebicka@ukmuenster.de

Funding information
Bundesministerium für Bildung und Forschung, Grant/Award Number: DEEP-HCC; Deutsche Forschungsgemeinschaft, Grant/Award Number: 403224013 -SFB 1382 (A09);

Abstract

Background and Aims: Janus kinase 2 (JAK2) signaling is increased in human and experimental liver fibrosis with portal hypertension. JAK2 inhibitors, such as pacritinib, are already in advanced clinical development for other indications and might also be effective in liver fibrosis. Here, we investigated the antifibrotic role of the JAK2 inhibitor pacritinib on activated hepatic stellate cells (HSCs) *in vitro* and in two animal models of liver fibrosis *in vivo*.

Abbreviations: Acta2, alpha-smooth muscle actin; ALT, alanine aminotransferase; ANOVA, analysis of variance; Arhgef1, Rho guanine nucleotide exchange factor 1; ASH, alcoholic steatohepatitis; AST, aspartate aminotransferase; AT1R, angiotensin-II-type-I receptor; bw, body weight; BrdU, bromodeoxyuridine; CCl4, carbon tetrachlorice; Col1a1, type I collagen; CSF1R, colony-stimulating factor 1 receptor; H&E, hematoxylin–eosin; HSC, hepatic stellate cell; i.v., intravenous; IRAK1, interleukin-1 receptor-associated kinase; JAK, Janus kinase; JAK2, Janus kinase 2; NASH, nonalcoholic steatohepatitis; Pcna, proliferating cell nuclear antigen; p-moesin, phospho-moesin; RHOA, Ras homolog family member A; ROCK, RHOA/Rho-kinase; $SM22^{Cre+}$-$Jak2^{f/f}$, floxed-Jak2 knockout mice with smooth muscle protein 22 Cre-promotor; SR, Sirius red; Tgfb, transforming growth factor beta; TGG, triglyceride; v:v, volume:volume; WD, Western diet; α-SMA, alpha-smooth muscle actin.

Sandra Torres and Cristina Ortiz shared first authorship.

Supplemental Digital Content is available for this article. Direct URL citations appear in the printed text and are provided in the HTML and PDF versions of this article on the journal's website, www.hepjournal.com.

Eurostars, Grant/Award Number: 12350; H2020 European Research Council, Grant/Award Number: 668031, 731875, 825694, 847949 and 964590; Hessian Ministry of Higher Education, Research and the Arts (HMWK)

Approach and Results: Transcriptome analyses of JAK2 in human livers and other targets of pacritinib have been shown to correlate with profibrotic factors. Although transcription of JAK2 correlated significantly with *type I collagen* expression and other profibrotic genes, no correlation was observed for *interleukin-1 receptor-associated kinase* and colony-stimulating factor 1 receptor. Pacritinib decreased gene expression of fibrosis markers in mouse primary and human-derived HSCs *in vitro*. Moreover, pacritinib decreased the proliferation, contraction, and migration of HSCs. C_{57}BL/6J mice received ethanol in drinking water (16%) or Western diet in combination with carbon tetrachloride intoxication for 7 weeks to induce alcoholic or nonalcoholic fatty liver disease. Pacritinib significantly reduced liver fibrosis assessed by gene expression and Sirius red staining, as well as HSC activation assessed by alpha-smooth muscle actin immunostaining in fibrotic mice. Furthermore, pacritinib decreased the gene expression of hepatic steatosis markers in experimental alcoholic liver disease. Additionally, pacritinib protected against liver injury as assessed by aminotransferase levels.

Conclusions: This study demonstrates that the JAK2 inhibitor pacritinib may be promising for the treatment of alcoholic and nonalcoholic liver fibrosis and may be therefore relevant for human pathology.

INTRODUCTION

Chronic liver injury, such as chronic viral infection, alcoholic steatohepatitis (ASH), and non-ASH (NASH), induces progressive fibrosis and may result in cirrhosis with portal hypertension.[1,2] The main profibrotic and procontractile cell types in the liver are the hepatic stellate cells (HSCs), which, once activated, produce excessive amounts of extracellular matrix, especially collagen.[3,4] Recently, we and others have shown that Janus kinase 2 (JAK2) is upregulated in human and murine HSCs and that it mediates fibrogenesis and contraction of HSCs downstream of the angiotensin-II-type-I receptor (AT1R).[5–9] Previously, we could show that Jak2 inhibition and overexpression have, respectively, blunted or enhanced liver fibrosis *in vitro* and *in vivo*.[5,6] The AT1R is coupled to JAK2, which in turn activates the Rho guanine nucleotide exchange factor 1 (Arhgef1)/Ras homolog family member A (RhoA)/Rho-kinase (ROCK) pathway, which is upregulated in human cirrhosis.[5,6] Pharmacological inhibition and genetic JAK2 deficiency blunted fibrogenesis and decreased portal pressure in different mouse models and decreased the contractility of HSCs *in vitro*.[5–7]

Interestingly, Janus kinase (JAK) inhibitors are already in clinical use for myelofibrosis, a bone marrow blood cancer characterized by increased inflammation and fibrosis.[10] Although the US Food and Drug Administration has approved two JAK inhibitors (ruxolitinib, fedratinib),[11] pacritinib is in advanced clinical development for myelofibrosis.[12–14] It is more specific for JAK2 than existing JAK inhibitors and does not induce myelosuppression.[15] Although pacritinib specifically inhibits JAK2, several studies indicate that it also can inhibit the signaling of the nontyrosine kinases interleukin-1 receptor-associated kinase (IRAK1) and colony-stimulating factor 1 receptor (CSF1R), which are involved in microenvironmental tumor interactions, as well as in tumor progression.[16–18]

In this study, we investigate the therapeutic role of the JAK2 inhibitor pacritinib in chronic liver disease with fibrosis. We show that pacritinib decreases the activation of HSC *in vitro* and that oral gavage of pacritinib ameliorates liver fibrosis progression in two experimental models of liver fibrosis with different etiologies *in vivo*.

MATERIALS AND METHODS

Human cell lines

Snap-frozen LX-2 cells (provided by V.S., Mayo Clinic) and TWNT-4 cells (provided by M.-L.B., RWTH Aachen),[19–21] both immortalized human-derived HSCs, were incubated with cell culture medium (Dulbecco's Modified Eagle Medium [DMEM] +10% fetal bovine serum +penicillin/streptomycin) in plastic flasks at 37°C.

After reaching 80% confluency, cells were passaged with a 1:2 split ratio.

Isolation of primary HSCs

HSCs of C_{57}BL/6J wild-type mice and floxed-Jak2 knockout mice with smooth muscle protein 22 Cre-promotor ($SM22^{Cre+}$-$Jak2^{f/f}$) were isolated as described previously.[5,22] Briefly, primary HSCs were isolated in a two-step pronase–collagenase liver perfusion from healthy mice by density gradient centrifugation. Viability and purity were systematically above 95%. Cells were seeded on uncoated plastic culture dishes. Experiments were performed 7 days after isolation or after the first passage (10 days) when HSCs were fully activated.

Pacritinib treatment *in vitro*

Human-derived (LX-2 and TWNT-4) and primary murine HSCs were incubated with 1 µm of pacritinib (SB1518, Cayman Chemical) diluted in DMEM +penicillin/streptomycin for 24 h and harvested for protein and gene expression analysis afterwards.

Mice

All experiments were approved and performed in accordance with the German animal protection law of the Animal Care and Use Committee Hesse, Germany, in the animal care facility (application number: V54-19c20/15-FK/2005). All animals received human care according to the criteria outlined in the EU regulations on animal research (2010/63/EU). Mice were purchased by Charles River Laboratories. $SM22^{Cre+}$-$Jak2^{f/f}$ breeding pairs were kindly provided by Peter Sayeski, Department of Physiology and Functional Genomics, University of Florida, College of Medicine. At the end of the experiments, sera and livers were collected for histological and molecular readouts of fibrosis, inflammation, and steatosis.

Toxic models of liver fibrosis in mice

ASH model

Male 10–12-week-old wild-type C_{57}BL/6J male mice were fed ad libitum for 7 weeks with ethanol in the drinking water (4% during week 1, 8% during week 2, and 16% until euthanized) and with normal chow (Sniff Spezialdäten GmbH). Mice were randomly divided into two groups: corn oil + ethanol group and carbon tetrachloride (CCl_4)/ethanol group. The intraperitoneal injection dose was 0.75 µl per g of body weight corn oil or 2 µl per g of body weight CCl_4 (CCl_4:corn oil = 1:3; volume:volume [v:v]) for 7 weeks (twice a week) to induce liver fibrosis.[23]

NASH model

Male 10–12-week-old wild-type C_{57}BL/6J mice were fed ad libitum for 7 weeks with high fat and cholesterol rich Western diet (WD) (diet #S0279-S011, 1.25% cholesterol, Sniff Spezialdäten GmbH). Mice were randomly divided into two groups: corn oil/WD group and CCl_4/WD group. The intraperitoneal injection dose was 0.75 µl per g of body weight corn oil or 2 µl per g of body weight CCl_4 (CCl_4:corn oil = 1:3; v:v) for 7 weeks (twice per week) to induce liver fibrosis.[23]

Pacritinib treatment *in vivo*

After 3 weeks of ASH- or NASH-induced liver injury, mice received pacritinib (SB1518, Cayman Chemical) either orally by gavage or by intravenous (i.v.) injection for an additional 4 weeks. Mice were gavaged with pacritinib (300mg/kg body weight) or vehicle three times per week for 3 more weeks. Another group of mice with CCl_4/ethanol-induced liver injury was injected with pacritinib (65 µg/kg body weight) or vehicle intravenously twice per week.

Transcriptome analysis

Transcriptome analyses were performed on whole liver samples of patients with cirrhosis ($n = 23$) and healthy individuals ($n = 7$) using the Illumina NovaSeq 6000 S4 reagent kit (200 cycles) with the NovaSeq Xp 4-Lane kit. The count matrix was generated using BioJupies,[24] data were normalized with the R package edgeR (version 3.30.0),[25] and differential gene expression analysis was performed with the R package limma (version 3.44.1).[26] Correlation analysis of whole liver samples was performed and visualized with the R package corrplot using the Spearman correlation method.[27] The local ethics committee of the University of Bonn approved the study (029/13), and all patients agreed and signed an informed written consent in accordance with the Declaration of Helsinki for the procedures they underwent.

Statistical analysis

Statistical analyses among groups were performed using Prism, version 5.0 (GraphPad). Data were expressed as mean ± SD for *in vitro* experiments and ± SEM for *in vivo* experiments. Comparisons between

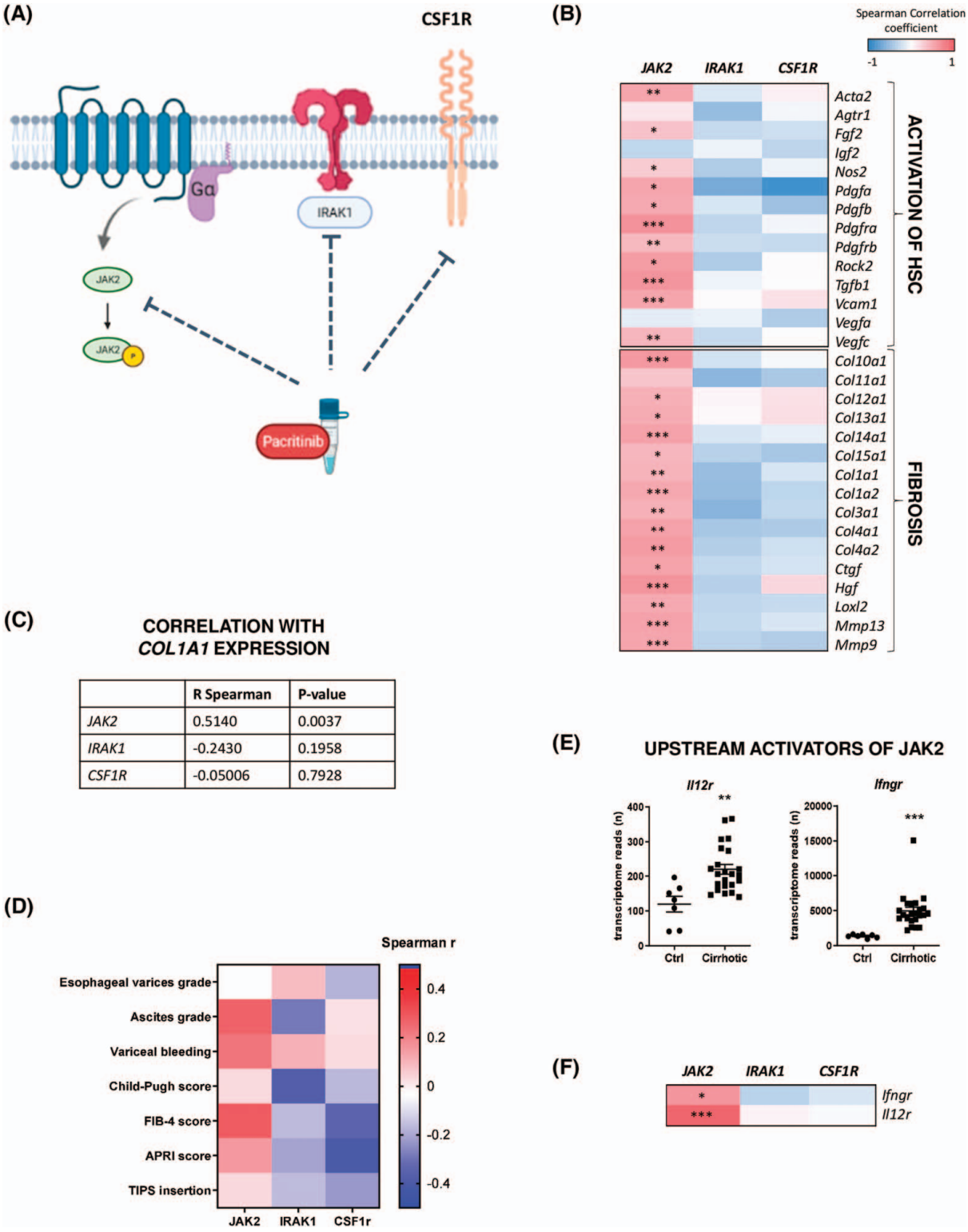

	R Spearman	P-value
JAK2	0.5140	0.0037
IRAK1	-0.2430	0.1958
CSF1R	-0.05006	0.7928

FIGURE 1 JAK2, the main target of pacritinib, correlates with fibrosis and portal hypertension in patients with cirrhosis. (A) Diagram of the pacritinib targets. (B) Heat map of the correlation among *Jak2*, *Irak1*, and *Csf1r* with genes associated to HSC activation and fibrosis. (C) Correlation of hepatic transcriptional levels of *Col1a1* with *Jak2*, *Irak1*, and *Csf1r*. (D) Heat map of correlation among *Jak2*, *Irak1*, and *Csf1r* with surrogates of portal hypertension. (E) Hepatic transcriptional levels of *Infgr* and *Il12*. (F) Heat map of correlation among *Jak2*, *Irak1*, and *Csf1r* with *Infgr* and *Il12*. Data are shown as Spearman rank coefficient (Rs) and *p* value. APRI, platelet ratio index; *Csf1r*, colony-stimulating factor 1 receptor; *Col1a1*, type I collagen; FIB-4, fibrosis-4 score; Gα, G protein alpha subunit; HSC, hepatic stellate cell; *Ifngr*, interferon-gamma receptor; *Il12r*, interleukin-12 receptor; *Irak1*, interleukin-1 receptor-associated kinase; JAK2, Janus kinase 2; TIPS, transjugular intrahepatic portosystemic shunt.

two groups were done by nonparametric Mann–Whitney U *t* tests. Comparisons among three and four groups were done with analysis of variance (ANOVA), followed by Tukey's multiple comparison posttest. A $p < 0.05$ was considered as significant ($^{\#}p < 0.1$, $^{*}p < 0.05$, $^{**}p < 0.01$, $^{***}p < 0.001$, $^{****}p < 0.0001$). All experiments were performed in triplicate at least three times, and representative images or blots are shown in the manuscript.

RESULTS

JAK2, the main target of pacritinib, correlates with fibrosis and portal hypertension in patients with cirrhosis

Although JAK2 is the main target of pacritinib, it might also target IRAK1 and CSF1R (Figure 1A). Therefore, we correlated the gene expression of these three kinases with the main gene markers of liver fibrosis and portal hypertension in patients with cirrhosis to identify their individual association with these processes. The clinical characteristics of patients with cirrhosis ($n = 23$) and noncirrhotic controls ($n = 7$) are presented in Table 1. The heat maps showed a strong correlation of *Jak2* with the genes associated with HSC activation and fibrosis, based upon Spearman's correlation coefficient for all analyzed genes (log2 fold) (Figure 1B), especially collagen-1 (Figure 1C), in patients with cirrhosis. Interestingly, *Irak1* and *Csf1r* showed negative correlations to those genes (Figure 1B) and were not correlated with type I collagen (*Col1a1*) (Figure 1C).

Portal hypertension is associated with the development of ascites and variceal bleeding, which could be reduced with the implantation of a transjugular intrahepatic portosystemic shunt (TIPS). Because we could not have a direct portal pressure measurement in these patients, we considered the presence of esophageal varices, ascites, variceal bleeding, Child–Pugh score, fibrosis-4 score, platelet ratio index score, and TIPS insertion in patients with cirrhosis as a surrogates of portal hypertension. To assess the correlation of portal hypertension with the expression of *Jak2, Irak1*, and *Csf1r*, we analyzed the correlation of the surrogate's grade with the expression of the three targets of pacritinib, and interestingly, *Jak2* correlates highly using portal hypertension surrogates in relation to *Irak1* and *Csf1r* (Figure 1D).

TABLE 1 General characteristics of patients

Parameters	Value
Patients (*n*)	30
Sex (female/male/no data)	7/16/7
Age (in years) as median (range)	46 (32–64)
Etiology (alcoholic/chronic hepatitis)	7/16
MELD score as median (range)	15 (6–23)
Child score as median (range)	9 (5–12)
Child category (A/B/C)	4/9/10
Ascites (absent/mild/severe)	19/6/5
Esophageal varices (absent/grade I–II/grade III–IV)	15/12/3

Abbreviation: MELD, model for end-stage liver disease.

Because JAK2 is activated in the liver by, inter alia, cytokines, we analyzed the expression of interferon-gamma receptor (*Ifngr*) and interleukin-12 receptor (*Il12r*), which were significantly increased in livers of patients with cirrhosis (Figure 1E).

We also analyzed their correlation with *Jak2*, *Irak1*, and *Csf1r* in livers of patients with cirrhosis (Figure 1F) and found that only *Jak2* was strongly correlated to *Il12r* and weakly to *Ifngr* in livers of patients with cirrhosis (Figure 1F). These results confirm our previous data,[5,6] namely, that the expression of *Jak2* is strongly associated with fibrosis progression and especially collagen in humans. Therefore, we used the JAK2 inhibitor pacritinib to assess its effects *in vitro* and *in vivo* experimental liver fibrotic models.

Pacritinib treatment JAK2-dependently blunts fibrogenesis and proliferation in rodent and immortalized human-derived HSCs

Because the main contributors to liver fibrosis are activated HSCs, isolated primary HSCs from wild-type and specific floxed-Jak2 knockout mice ($SM22^{Cre+}$-$Jak2^{f/f}$) were used to assess the effect of pacritinib. Therefore, HSCs with clearly activated phenotype after 7 days of culture growth were incubated with pacritinib.

First, we assessed protein levels and mRNA expressions of collagen-1, the main profibrotic marker, which were significantly reduced by pacritinib treatment and blunted in $SM22^{Cre+}$-$Jak2^{f/f}$ mouse HSCs (Figure 2A). We also assessed phospho-moesin (p-moesin) protein levels, which showed the same effect as in collagen-1 expression (Figure 2A). Moreover, we analyzed the related profibrotic genes, *Jak2*, *Rock*, alpha-smooth muscle actin (*Acta2*), and transforming growth factor beta (*Tgfb*), which showed a clear reduction after pacritinib incubation in wild-type and $SM22^{Cre+}$-$Jak2^{f/f}$ mouse HSCs (Figure 2B).

To confirm the results from rodent HSCs, we used two well-characterized human HSC lines (LX-2 and TWNT-4) to investigate the role of pacritinib *in vitro*. First, we analyzed mRNA expression and protein levels of collagen-1, and the results showed a significant decrease after pacritinib treatment in both human HSC lines (Figure 2C). The p-moesin protein levels showed the same outcome (Figure 2C). Furthermore, pacritinib reduced the expression of other genes related to HSC activation, such as *Tgfb* and platelet-derived growth factor

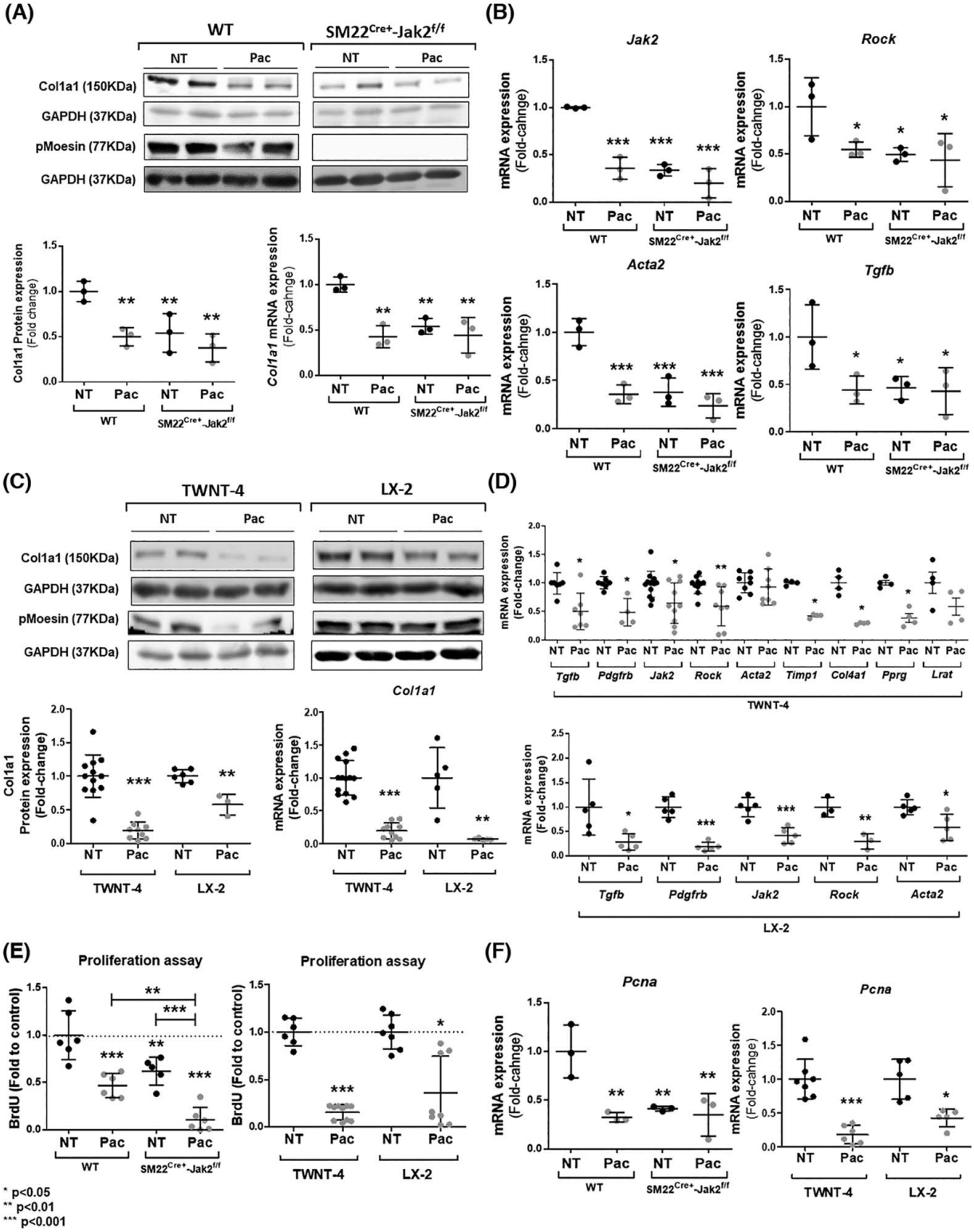

FIGURE 2 Pacritinib treatment JAK2-dependently blunts fibrogenesis and proliferation in rodent and immortalized human-derived HSCs. Isolated wild-type and SM22^{Cre+}-Jak2$^{f/f}$ mice HSCs were treated with pacritinib at 1 μm during 24 h to measure Col1a1 and p-moesin protein levels and Col1a1 gene expression (A) and mRNA expression levels of *Jak2*, *Rock*, *Acta2*, and *Tgfb* (B). TWNT-4 and LX-2 human HSCs were treated with pacritinib at 1 μm for 24 h to measure Col1a1 and p-moesin protein levels and Col1a1 gene expression (C) and mRNA expression of *Tgfb*, *Pdgfrb*, *Jak2*, *Rock*, and *Acta2* in TWNT-4 and LX2 and *Timp1*, *Col4a1*, *Pprg*, and *Lrat* in TWNT-4 (D). BrdU proliferation assay (E); *Pcna* mRNA expression (F). Results are expressed as the mean ± standard deviation; $^{\#}p < 0.1$. $^{*}p < 0.05$, $^{**}p < 0.01$, and $^{***}p < 0.001$. *Acta2*, alpha-smooth muscle actin; BrdU, bromodeoxyuridine; Col1a1, type I collagen; *Col4a1*, collagen-IV; GAPDH, glyceraldehyde-3-phosphate dehydrogenase; HSC, hepatic stellate cell; Jak2, Janus kinase 2; *Lrat*, lecithin-retinol acyltransferase; NT, nontreated; Pac, pacritinib; *Pdgfrb*, platelet-derived growth factor receptor beta; p-moesin, phospho-moesin; Pprg, peroxisome proliferator activated receptor gamma; *Rock*, RhoA/Rho-kinase; SM22^{Cre+}-Jak2$^{f/f}$, floxed-Jak2 knockout mice with smooth muscle protein 22 Cre-promotor; *Tgfb*, transforming growth factor beta; *Timp1*, tissue inhibitor of metalloproteinases 1; WT, wild type.

receptor beta, and components of the AT1R pathway, such as *JAK2* and *Rock*, in both cell lines (Figure 2D). *Acta2* was only significantly reduced in LX-2 HSCs (Figure 2D). Moreover, we analyzed other fibrogenic targets, such as tissue inhibitor of metalloproteinases 1, collagen-IV, peroxisome proliferator activated receptor gamma, and lecithin-retinol acyltransferase (*Lrat*) in TWNT-4 cells (Figure 2D), which, except for *Lrat*, showed a significant reduction after pacritinib treatment.

Next, we evaluated the proliferation capacity in rodent HSCs and in both human cell lines with or without pacritinib incubation. Our findings show that pacritinib reduced bromodeoxyuridine (BrdU) proliferation assay and the gene expression levels of the proliferation marker proliferating cell nuclear antigen (*Pcna*) (Figure 2E,F). Similar effects were observed in $SM22^{Cre+}$-$Jak2^{f/f}$ mouse HSCs with minor but significant changes after pacritinib treatment (Figure 2E,F).

Jak2 inhibition with pacritinib treatment reduces contraction and migration of rodent and immortalized human-derived HSCs.

To further underline the effects of pacritinib on HSC activation, we assessed the contraction capacity in rodent and both human cell lines, which resulted in a significant relaxation of rodent HSCs treated with pacritinib and also in $SM22^{Cre+}$-$Jak2^{f/f}$ HSC (Figure 3A). Pacritinib-treated activated TWNT-4 and LX-2 cells were less contractile than nontreated cells (Figure 3A).

After showing the effect of JAK2 inhibition on fibrogenesis, proliferation, and contraction, we evaluated their migration ability. To measure the migration ability, we performed the wound-healing assay. Although the nontreated cells closed the gap, pacritinib-treated cells showed decreased migration, and a larger gap remained (Figure 3B). Migration ability was significantly reduced in nontreated and treated $SM22^{Cre+}$-$Jak2^{f/f}$ mice HSCs with pacritinib (Figure 3B), indicating no additional effect. Collectively, these findings indicated that pacritinib in $SM22^{Cre+}$-$Jak2^{f/f}$ mice significantly reduces the activation of HSC, demonstrated by reduced fibrogenesis, proliferation, contraction, and migration. This underlines the potential therapeutic effect of pacritinib on the key hepatic cell type that contributes to liver fibrosis progression.

Intravenous pacritinib administration ameliorates CCl_4/ethanol-induced liver fibrosis in mice

To better understand the observed effects of pacritinib *in vitro*, we assessed the effect of JAK2 inhibition on hepatic fibrogenesis in an ASH model with liver fibrosis, which mimics chronic alcohol abuse, one of the main causes of chronic liver disease that can further progress to liver fibrosis. Wild-type mice were treated with ethanol in their drinking water or in combination with CCl_4 intoxications for 7 weeks. We evaluated the effect of pacritinib administered by i.v. injection (65 µg/kg body weight [bw], twice per week) starting 3 weeks after the first CCl_4 injection for a further 4 weeks (Figure S1A}.

After induction of liver fibrosis by CCl_4/ethanol, pacritinib i.v. treatment showed a significant reduction in serum alanine aminotransferase (ALT) levels (Figure S1B) and aspartate aminotransferase (AST) levels (Figure S1C). Hematoxylin–eosin (H&E) stainings showed an improvement in the liver parenchyma after pacritinib treatment (Figure S1D, upper panel).

Next, we examined hepatic fibrosis by Sirius red (SR) stainings of collagen fibers and the activation of HSCs by alpha-smooth muscle actin (α-SMA) immunohistochemistry stainings. The results showed a significant decrease in SR stainings with pacritinib treatment (Figure S1D, middle panel) and a trend toward reduction in α-SMA immunostaining (Figure S1D, lower panel). Furthermore, pacritinib significantly reduced collagen-1 and p-moesin, which is a surrogate for ROCK activity (Figure S1 E). Additionally, a trend toward reduction was shown in *Col1a1* mRNA expression with pacritinib treatment, whereas no significant changes in *Acta2* and *Tgfb* were observed (Figure S1F).

Given that alcohol consumption increases liver triglyceride and fat droplet accumulation, we assessed hepatic steatosis by analysis of mRNA expression levels of central regulators of lipid homeostasis, sterol regulatory element binding factor 1c (*Srebp1c*), and fatty acid synthase (*Fasn*) and the presence of small lipid droplets by oil red O staining, quantitative hepatic triglyceride (TGG) content, and liver-to-body weight ratio. The results revealed no changes with the pacritinib i.v. treatment (Figures S1G and S2A–C). These results suggest that i.v. pacritinib treatment reduces liver fibrosis but does not cause changes in steatosis.

Therapeutic approach of pacritinib in CCl_4/ethanol-induced liver fibrosis in mice

Next, we examined whether oral administration of pacritinib (300mg/kg bw, three times per week) is as effective as i.v. administration because this is the route of administration in clinics (Figure 4A).

Oral pacritinib treatment reduced ALT and AST levels (Figure 4B,C), which paralleled the reduced liver injury observed by H&E after pacritinib treatment (Figure 4D, upper panel). In addition, we analyzed the levels of inflammatory (*Ccl2*) and proliferative markers (*Pcna*), and the results showed a significative reduction

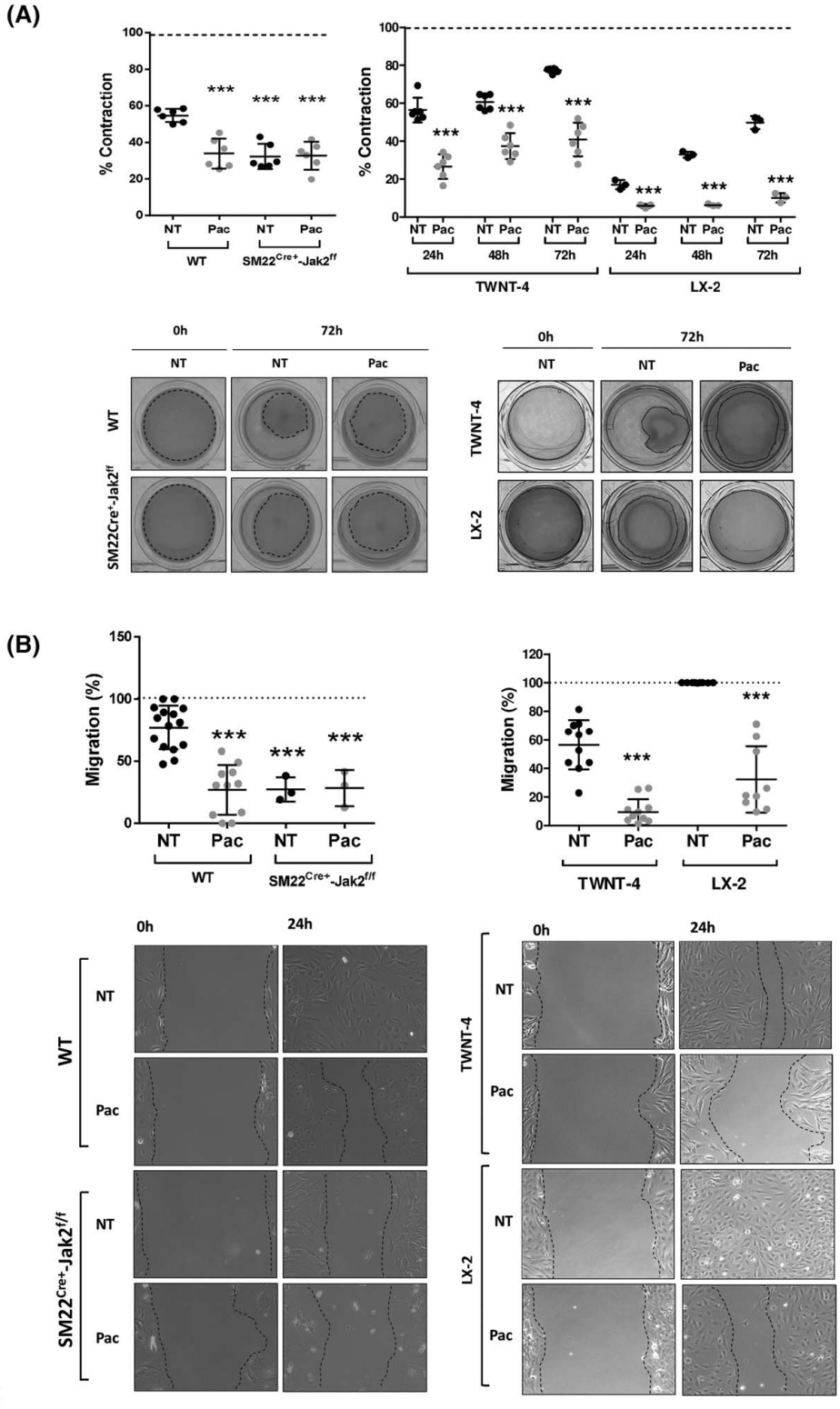

FIGURE 3 JAK2 inhibition with pacritinib treatment reduces contraction and migration of rodent and immortalized human-derived HSCs. (A) Quantification and representative images of contraction assay at 72 h, and (B) scratch assay quantification and representative pictures (B) at 24 h. Results are expressed as the mean ± standard deviation; $^{\#}p < 0.1$. $^{*}p < 0.05$, $^{**}p < 0.01$, and $^{***}p < 0.001$. HSC, hepatic stellate cell; JAK2, Janus kinase 2; SM22^{Cre+}-Jak2$^{f/f}$, floxed-Jak2 knockout mice with smooth muscle protein 22 Cre-promotor; NT, nontreated; Pac, pacritinib; WT, wild type.

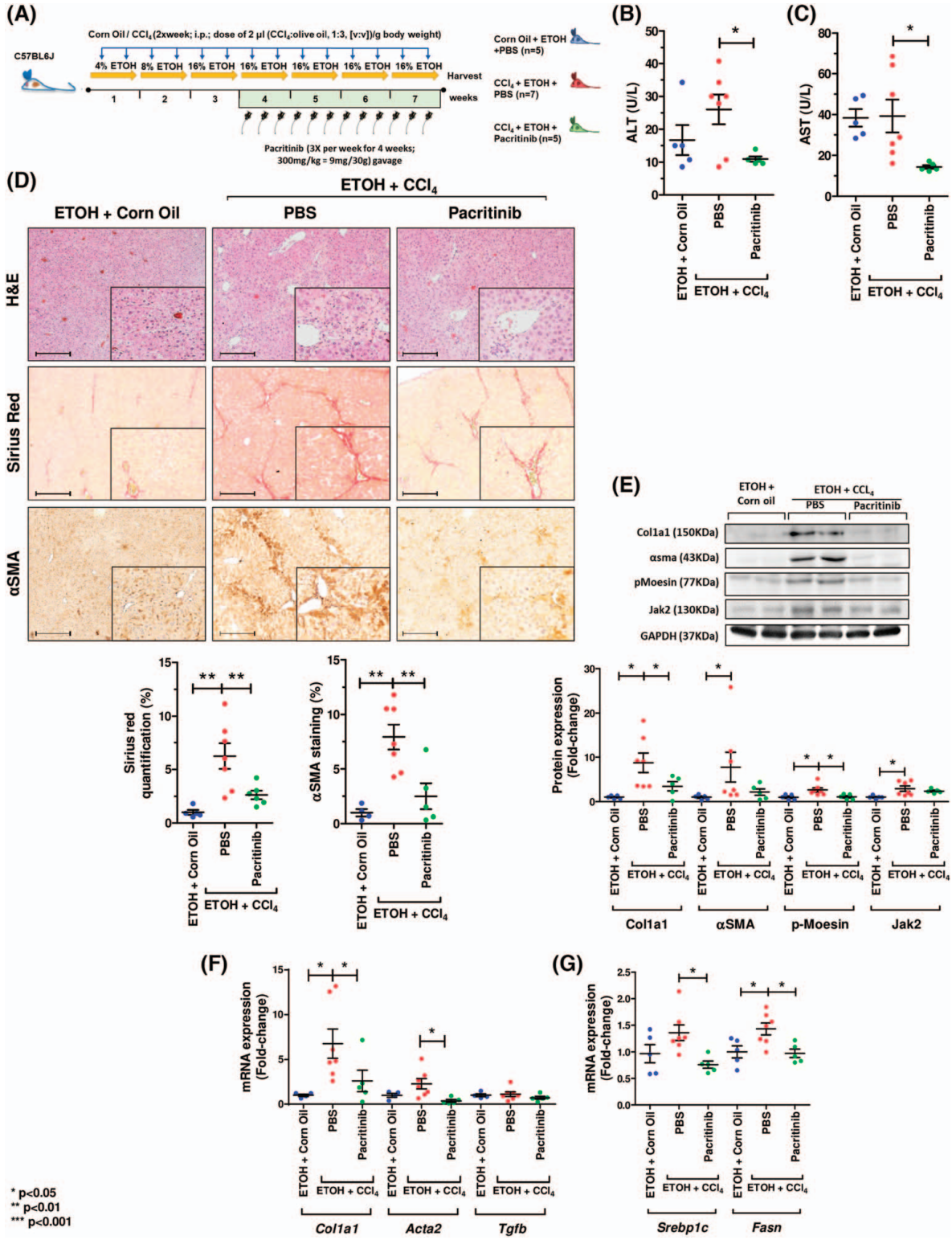

FIGURE 4 Therapeutic approach of pacritinib in CCl_4/ethanol-induced liver fibrosis in mice. Experimental design (A), serum aminotransferases levels ALT (B) and AST (C), hematoxylin and eosin (H&E), Sirius red staining and α-SMA immunohistochemistry representative images and quantifications (D), protein levels (E) and mRNA expression (F) of fibrotic markers. *Srebp1c* and *Fasn* gene expression (G). Results are expressed as the mean ± SEM; $^{\#}p < 0.1$, $^{*}p < 0.05$, $^{**}p < 0.01$, and $^{***}p < 0.001$. Representative photomicrographs were captured at 100× (scale bars = 200 µm) and 200× magnification (scale bars = 100 µm). α-SMA, alpha-smooth muscle actin; *Acta2*, alpha-smooth muscle actin; ALT, alanine aminotransferase; AST, aspartate aminotransferase; CCl_4, carbon tetrachloride; Col1a1, type I collagen; ETOH, ethanol; *Fasn*, fatty acid synthase; GAPDH, glyceraldehyde-3-phosphate dehydrogenase; Jak2, Janus kinase 2; p-moesin, phospho-moesin; Srebp1c, sterol regulatory element binding factor 1; *Tgfb*, transforming growth factor beta; v:v, volume:volume.

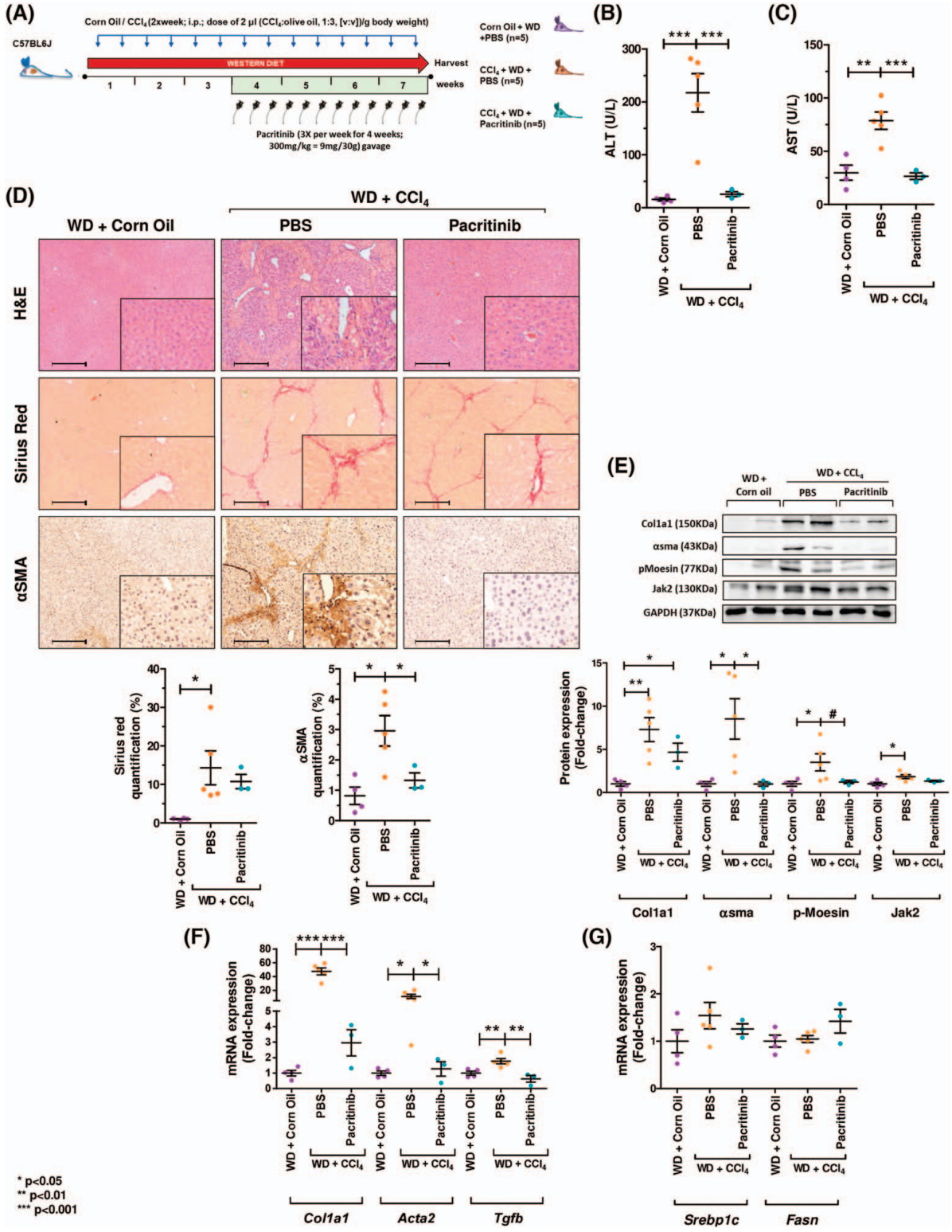

FIGURE 5 Oral pacritinib treatment reduces the progression of CCl_4/WD-induced liver fibrosis in mice. Experimental design (A), serum aminotransferases levels ALT (B) and AST (C), hematoxylin and eosin (H&E), Sirius red staining and α-SMA immunohistochemistry representative images and quantifications (D), protein levels (E), and mRNA expression (F) of fibrotic markers. *Srebp1c* and *Fasn* gene expression (G). Results are expressed as the mean ± SEM; $^{\#}p < 0.1$, $^{+}p < 0.05$, $^{**}p < 0.01$, and $^{***}p < 0.001$. Representative photomicrographs were captured at 100× (scale bars = 200 µm) and 200× magnification (scale bars = 100 µm). α-SMA, alpha-smooth muscle actin; *Acta2*, alpha-smooth muscle actin; ALT, alanine aminotransferase; AST, aspartate aminotransferase; CCl_4, carbon tetrachloride; Col1a1, type I collagen; *Fasn*, fatty acid synthase; GAPDH, glyceraldehyde-3-phosphate dehydrogenase; Jak2, Janus kinase 2; *Srebp1c*, sterol regulatory element binding factor 1; *Tgfb*, transforming growth factor beta; v:v, volume:volume; WD, Western diet.

after pacritinib treatment in *Ccl2* gene expression (Figures S3 and S4D). F4/80 and Terminal deoxynucleotidyl transferase (TdT) dUTP Nick-End Labeling (TUNEL) staining showed a significant reduction with oral pacritinib treatment in fibrotic mice (Figure S4E,F). SR stainings and α-SMA immunohistochemistry quantifications revealed a significant reduction after pacritinib treatment (Figure 4D, middle and lower panel). These findings were accompanied by decreased protein levels of collagen-1 and p-moesin and with a trend toward reduction in α-SMA and Jak2 (Figure 4E). Also, mRNA expression of *Col1a1* and *Acta2* showed a significant reduction (Figure 4F). Liver fibrosis was further evaluated by extracellular volume fraction (ECV) using quantitative magnetic resonance imaging mapping. Representative images of ECV showed a significant increase in fibrotic animals compared with the control group, and this effect was prevented with pacritinib treatment (Figure S4A). Portal pressure was measured and showed a significant reduction with oral pacritinib treatment in fibrotic mice (Figure S4C).

Additionally, significant changes were observed in mRNA expression of *Srebp1c* and *Fasn* steatosis markers (Figure 4G). Although no changes were observed in TGG hepatic content, a significant reduction was shown in oil red O staining and liver-to-body weight ratio after oral pacritinib treatment (Figure S2A–C), indicating that oral pacritinib has an effect on hepatic steatosis in alcoholic liver fibrosis in mice. Finally, regarding the effect of pacritinib on JAK/signal transducer and activator of transcription (STAT) signaling, we tested phospho-STAT 3 (pSTAT3) and pSTAT5 in this experimental model, but no major impact was observed in STAT phosphorylation proteins (Figure S5). Thus, our data indicate that pacritinib treatment has beneficial effects on liver fibrosis in ASH murine models.

Oral pacritinib treatment reduces the progression of CCl_4/WD-induced liver fibrosis in mice

Finally, we studied the effects of pacritinib in a NASH model, using a combination of CCl_4/WD, which induces liver fibrosis within 7 weeks. During the last 4 weeks, NASH mice were treated with pacritinib by oral gavage (300mg/kg bw, three times per week), based on the results observed in the ASH model (Figure 5A).

Elevations of serum ALT and AST due to CCl_4/WD decreased in groups treated with pacritinib (Figure 5B,C). Pacritinib protection against the NASH model was also shown in H&E staining (Figure 5D, upper panel). At the same time, we analyzed the gene expression of inflammation (*Ccl2*) and proliferative (*Pcna*) markers, whereby only the inflammation marker was decreased after pacritinib treatment (Figures S3 and S4D). In line with these results, F4/80 and TUNEL staining showed the same outcome (Figure 4E,F). SR staining showed a trend toward decreased collagen-1 deposition after pacritinib treatment (Figure 4D, middle panel). Nevertheless, representative images of α-SMA immunohistochemistry and quantification of the α-SMA-positive tissue area (Figure 4D, lower panel) showed protection after pacritinib treatment compared with CCl_4/WD-treated mice. These data were accompanied by collagen-1, α-SMA, and p-moesin protein expression, which revealed a tendency toward decrease after pacritinib treatment (Figure 4E). Quantitative PCR of the fibrotic genes *Col1a1*, *Acta2*, and *Tgfb* confirmed the protein results of reduced expression after pacritinib treatment (Figure 4F).

However, no changes in mRNA expression of steatosis markers were observed in the NASH model treated with pacritinib (Figure 4G). In addition to these findings, no changes were shown in oil red O stainings, TGG content, and liver-to-body weight ratios (Figure S2D–F). Finally, regarding the effect of pacritinib on JAK/STAT signaling, the same results were observed in STAT phosphorylation proteins in the NASH model (Figure S5). Overall, these results suggest that pacritinib treatment reduces fibrosis development in the NASH mouse model without changes in lipid accumulation.

DISCUSSION

n this study, we assessed the antifibrotic effect of the JAK2 inhibitor pacritinib *in vitro* in murine and human HSCs and *in vivo* in ASH and NASH murine models. Pacritinib is a type 1 inhibitor of JAKs, which targets the ATP binding site of the JAK2 under active conformation of the kinase domain.[16,28] To date, three clinical trials to test pacritinib for the treatment of myelofibrosis (phase 3 PERSIST-1 and PERSIST-2 trials and phase 2 PAC203 trials) have been completed.[29–31] It is known that pacritinib does not induce myelosuppression and exerts less immunosuppressive properties than other JAK inhibitors, therefore having the potential to be used in combination with established therapies for the treatment of other inflammatory diseases.[16]

Our previous findings demonstrated that the AT1R/JAK2/ROCK pathway is induced in patients with portal hypertension and decompensation in cirrhosis.[5,6] In line with other findings,[9] we confirm the correlation of *Jak2* and *Col1a1* in patients with cirrhosis in relation to liver fibrosis and portal hypertension. Interestingly, among the pacritinib targets, only JAK2 shows correlation with liver fibrosis and activation of HSC-related genes in patients with cirrhosis. These results confirm the role of JAK2 in activated HSCs, as well as its effect on fibrosis progression.[5,6] Importantly, Jak2 expression and phosphorylation were particularly common in HSCs.[5] Additionally, our previous finding showed that inhibition of JAK2 using AG490 decreased hepatic resistance and thereby portal pressure in these animals, indicating that JAK2 plays an important role in portal hypertension.[7]

Another study demonstrated that selective inhibition of JAK2, with the antagonist TG101348 (fedratinib), not only blunted HSC activation but also macrophage-driven inflammation in NASH, both *in vitro* and *in vivo*.[9] Moreover, mice with hepatocyte-specific deletion of JAK2 were protected from diet-induced steatohepatitis, insulin resistance, and liver carcinogenesis.[32,33]

In this study, we report that the JAK2 inhibitor pacritinib reduces proliferation, migration, contraction, and gene and protein expression from fibrosis markers in two human-derived HSCs and primary murine HSCs. In line with these *in vitro* findings, we treated the following two mouse models of chronic liver disease with pacritinib: the CCl_4/ethanol model to mimic ASH, which induces fibrosis, inflammation, and steatosis, and the CCl_4/WD model to mimic NASH, with a rapid progression of steatohepatitis, obesity, slight inflammation, and fibrosis. Pacritinib treatment was able to blunt or interrupt liver fibrosis development in ASH and NASH mouse models, assessed by SR stainings. HSC activation was assessed by α-SMA immunostaining and the expression of fibrotic markers. Furthermore, pacritinib decreased hepatic steatosis markers in the ASH model, which may be explained either by reduction in ROS-induced lipid peroxidation, protein oxidation, and consequently a reduction in DNA damage[34,35] or by the anti-inflammatory effect. Consequently, pacritinib decreased liver injury–induced aminotransferase levels in both experimental fibrotic models, suggesting that pacritinib significantly improved liver function and that it is not toxic in liver disease. Curiously, we observed that the levels of Jak2 mRNA and protein decreased with pacritinib; such as in other studies, it could be a feedforward mechanism[36] or an autoinhibition mechanism.[37] Moreover, other studies suggest that the inhibitory functions of Tyr kinase domain JAK homogy 2 (JH2) kinase domain of Jak kinases are important for maintaining Jak2 in a low-activity state in the absence of ligand stimulation; autoinhibitory domains also have been proposed.[38] However, the complexity of the three-dimensional structure of Jak kinases and the different interactions of the two kinase domains (JH1 and JH2)[38] have not been clearly defined. In conclusion, we provide evidence that pacritinib could be a potential for therapy in patients with liver fibrosis.

AUTHOR CONTRIBUTIONS

Jonel Trebicka, Sabine Klein, and Sandra Torres drafted the manuscript. Sabine Klein, Sandra Torres, Cristina ortiz, Nadine Bachtler, Wenyi Gu, Leon D. Grünewald, Nico Kraus, Robert Schierwagen, Christoph Hieber, Caroline Meier, Olaf Tyc, Frank Erhard Uschner, Jose Carlos Fernandez-Checa, Carmen Garcia-Ruiz, Thomas J. Vogl, Christian Trautwein, Marie-Luise Berres, Christoph Welsch, analyzed and interpreted the data. Jonel Trebicka, Sabine Klein, Bart Nijmeijer, Stefan Zeuzem, and Sandra Torres designed the original study, interpreted the data, and supervised and obtained financial support for the study. All authors reviewed the draft for important intellectual content and approved the final article for submission.

ACKNOWLEDGMENTS

All the authors are very grateful to Dikra Zouiten and Evelin Süß for their excellent technical assistance and Dr. Vijay Shah (V.S.) for providing the LX-2 cells.

FUNDING INFORMATION

Jonel Trebicka is supported by the German Research Foundation project ID 403224013–SFB 1382 (A09); by the German Federal Ministry of Education and Research (BMBF) for the DEEP-HCC project; by the Hessian Ministry of Higher Education, Research, and the Arts (HMWK) for the ENABLE cluster project; and by Eurostars (Grant ID 12350). The MICROB-PREDICT (project ID 825694), DECISION (project ID 847949), GALAXY (project ID 668031), LIVERHOPE (project ID 731875), and IHMCSA (project ID 964590) projects have received funding from the European Union's Horizon 2020 research and innovation program. The manuscript reflects only the authors' views, and the European Commission is not responsible for any use that may be made of the information it contains. The funders had no influence on study design, data collection and analysis, decision to publish, or preparation of the manuscript.

CONFLICT OF INTEREST

Stefan Zeuzem consults for and is on the speakers' bureau for Gilead and BioMarin. He consults for NovoNordisk and GSK. Jonel Trebicka has received speaking and/or consulting fees from Versantis, Gore, Boehringer-Ingelheim, Alexion, Falk, Mallinckrodt, Grifols and CSL Behring.

ORCID

Sandra Torres https://orcid.org/0000–0002–2894–3188
Olaf Tyc https://orcid.org/0000–0001–9949–0975
Jonel Trebicka https://orcid.org/0000–0002–7028–3881

REFERENCES

1. Bataller R, Brenner DA. Liver fibrosis. J Clin Invest. 2005;115:209–18.
2. Gu W, Hortlik H, Erasmus HP, Schaaf L, Zeleke Y, Uschner FE, et al. Trends and the course of liver cirrhosis and its complications in Germany: Nationwide population-based study (2005 to 2018). Lancet Reg Health Eur. 2021;12:100240.
3. Liedtke C, Luedde T, Sauerbruch T, Scholten D, Streetz K, Tacke F, et al. Experimental liver fibrosis research: update on animal models, legal issues and translational aspects. Fibrogenesis Tissue Repair. 2013;6:19.
4. Ortiz C, Schierwagen R, Schaefer L, Klein S, Trepat X, Trebicka J. Extracellular matrix remodeling in chronic liver disease. Curr Tissue Microenviron Rep. 2021;2:41–52.
5. Granzow M, Schierwagen R, Klein S, Kowallick B, Huss S, Linhart M, et al. Angiotensin-II type 1 receptor-mediated Janus kinase 2 activation induces liver fibrosis. Hepatology. 2014;60:334–48.

6. Klein S, Rick J, Lehmann J, Schierwagen R, Schierwagen IG, Verbeke L, et al. Janus-kinase-2 relates directly to portal hypertension and to complications in rodent and human cirrhosis. Gut. 2015;66:145–55.
7. Klein S, Kleine CE, Pieper A, Granzow M, Gautsch S, Himmit M, et al. TGR(mREN2)27 rats develop non-alcoholic fatty liver disease-associated portal hypertension responsive to modulations of Janus-kinase 2 and Mas receptor. Sci Rep. 2019;9:11598.
8. Klein S, Frohn F, Magdaleno F, Reker-Smit C, Schierwagen R, Schierwagen I, et al. Rho-kinase inhibitor coupled to peptide-modified albumin carrier reduces portal pressure and increases renal perfusion in cirrhotic rats. Sci Rep. 2019;9:2256.
9. Akcora BÖ, Dathathri E, Ortiz-Perez A, Gabriël AV, Storm G, Prakash J, et al. TG101348, a selective JAK2 antagonist, ameliorates hepatic fibrogenesis in vivo. FASEB J. 2019;33:9466–75.
10. Zahr AA, Salama ME, Carreau N, Tremblay D, Verstovsek S, Mesa R, et al. Bone marrow fibrosis in myelofibrosis: pathogenesis, prognosis and targeted strategies. Haematologica. 2016;101:660–71.
11. Rudolph J, Heine A, Quast T, Kolanus W, Trebicka J, Brossart P, et al. The JAK inhibitor ruxolitinib impairs dendritic cell migration via off-target inhibition of ROCK. Leukemia. 2016;30:2119–23.
12. Singer JW, Al-Fayoumi S, Taylor J, Velichko S, O'Mahony A. Comparative phenotypic profiling of the JAK2 inhibitors ruxolitinib, fedratinib, momelotinib, and pacritinib reveals distinct mechanistic signatures. PLoS One. 2019;14:e0222944.
13. Duong VH, Komrokji RS. The role of pacritinib in the management of myelofibrosis. Exp Rev Hematol. 2014;7:325–32.
14. Rao TN, Hansen N, Hilfiker J, Rai S, Majewska JM, Leković D, et al. JAK2-mutant hematopoietic cells display metabolic alterations that can be targeted to treat myeloproliferative neoplasms. Blood. 2019;134:1832–46.
15. Al-Fayoumi S, Hashiguchi T, Shirakata Y, Mascarenhas J, Singer JW. Pilot study of the antifibrotic effects of the multikinase inhibitor pacritinib in a mouse model of liver fibrosis. J Exp Pharmacol. 2018;10:9–17.
16. Singer JW, Al-Fayoumi S, Ma H, Komrokji RS, Mesa R, Verstovsek S. Comprehensive kinase profile of pacritinib, a nonmyelosuppressive janus kinase 2 inhibitor. J Exp Pharm. 2016;8:11–9.
17. Hume DA, MacDonald KPA. Therapeutic applications of macrophage colony-stimulating factor-1 (CSF-1) and antagonists of CSF-1 receptor (CSF-1R) signaling. Blood. 2012;119:1810–20.
18. Singer JW, Fleischman A, Al-Fayoumi S, Mascarenhas JO, Yu Q, Agarwal A. Inhibition of interleukin-1 receptor-associated kinase 1 (IRAK1) as a therapeutic strategy. Oncotarget. 2018;9:33416–39.
19. Shibata N, Watanabe T, Okitsu T, Sakaguchi M, Takesue M, Kunieda T, et al. Establishment of an immortalized human hepatic stellate cell line to develop antifibrotic therapies. Cell Transplant. 2003;12:499–507.
20. Hicks DF, Goossens N, Blas-García A, Tsuchida T, Wooden B, Wallace MC, et al. Transcriptome-based repurposing of apigenin as a potential anti-fibrotic agent targeting hepatic stellate cells. Sci Rep. 2017;7:42563.
21. Qu C, Zheng D, Li S, Liu Y, Lidofsky A, Holmes JA, et al. Tyrosine kinase SYK is a potential therapeutic target for liver fibrosis. Hepatology. 2018;68:1125–39.
22. Weiskirchen S, Tag CG, Sauer-Lehnen S, Tacke F, Weiskirchen R. Isolation and culture of primary murine hepatic stellate cells. Methods Mol Biol. 2017;1627:165–91.
23. Brol MJ, Rösch F, Schierwagen R, Magdaleno F, Uschner FE, Manekeller S, et al. Combination of CCL4 with alcoholic and metabolic injuries mimics human liver fibrosis. Am J Physiol Gastrointest Liver Physiol. 2019;317:G182–94.
24. Torre D, Lachmann A, Ma'ayan A. BioJupies: automated generation of interactive notebooks for RNA-seq data analysis in the cloud. Cell Syst. 2018;7:556–61.e3.
25. Robinson MD, McCarthy DJ, Smyth GK. edgeR: a Bioconductor package for differential expression analysis of digital gene expression data. Bioinformatics. 2010;26:139–40.
26. Ritchie ME, Phipson B, Wu D, Hu Y, Law CW, Shi W, et al. Limma powers differential expression analyses for RNA-sequencing and microarray studies. Nucleic Acids Res. 2015;43:e47.
27. Wei T, Simko V. corrplot: Visualization of a correlation matrix. R package version 0.73. 2013;230(231):11. [cited 2020 Nov 27]. Available from: https://github.com/taiyun/corrplot
28. Vainchenker W, Leroy E, Gilles L, Marty C, Plo I, Constantinescu SN. JAK inhibitors for the treatment of myeloproliferative neoplasms and other disorders. F1000Res. 2018;7:82.
29. Gerds AT, Savona MR, Scott BL, Talpaz M, Egyed M, Harrison CN, et al. Determining the recommended dose of pacritinib: results from the PAC203 dose-finding trial in advanced myelofibrosis. Blood Adv. 2020;4:5825–35.
30. Mascarenhas J, Hoffman R, Talpaz M, Gerds AT, Stein B, Gupta V, et al. Pacritinib vs best available therapy, including ruxolitinib, in patients with myelofibrosis: a randomized clinical trial. JAMA Oncol. 2018;4:652–9.
31. Mesa RA, Vannucchi AM, Mead A, Egyed M, Szoke A, Suvorov A, et al. Pacritinib versus best available therapy for the treatment of myelofibrosis irrespective of baseline cytopenias (PERSIST-1): an international, randomised, phase 3 trial. Lancet Haematol. 2017;4:e225–36.
32. Shi SY, García Martin R, Duncan RE, Choi D, Lu SY, Schroer SA, et al. Hepatocyte-specific deletion of Janus kinase 2 (JAK2) protects against diet-induced steatohepatitis and glucose intolerance. J Biol Chem. 2012;287:10277–88.
33. Shi SY, Luk CT, Schroer SA, Kim MJ, Dodington DW, Sivasubramaniyam T, et al. Janus kinase 2 (JAK2) dissociates hepatosteatosis from hepatocellular carcinoma in mice. J Biol Chem. 2017;292:3789–99.
34. Themanns M, Mueller KM, Kessler SM, Golob-Schwarzl N, Mohr T, Kaltenecker D, et al. Hepatic deletion of janus kinase 2 counteracts oxidative stress in mice. Sci Rep. 2016;6:34719.
35. Kaltenecker D, Themanns M, Mueller KM, Spirk K, Suske T, Merkel O, et al. Hepatic growth hormone - JAK2 - STAT5 signalling: metabolic function, non-alcoholic fatty liver disease and hepatocellular carcinoma progression. Cytokine. 2019;124:154569.
36. Udhane V, Maranto C, Hoang DT, Gu L, Erickson A, Devi S, et al. Enzalutamide-induced feed-forward signaling loop promotes therapy-resistant prostate cancer growth providing an exploitable molecular target for Jak2 inhibitors. Mol Cancer Ther. 2020;19:231–46.
37. Kemp BE, Parker MW, Hu S, Tiganis T, House C. Substrate and pseudosubstrate interactions with protein kinases: determinants of specificity. Trends Biochem Sci. 1994;19:440–4.
38. Saharinen P, Takaluoma K, Silvennoinen O. Regulation of the Jak2 tyrosine kinase by its pseudokinase domain. Mol Cell Biol. 2000;20:3387–95.

How to cite this article: Torres S, Ortiz C, Bachtler N, Gu W, Grünewald LD, Kraus N, et al. Janus kinase 2 inhibition by pacritinib as potential therapeutic target for liver fibrosis. Hepatology. 2023;77:1228–1240. https://doi.org/10.1002/hep.32746